Influence of the rail dampers on the frequency-domain response of the rail

Traian Mazilu[1,*] and *Dorina* Fologea[2]

[1]University Politehnica of Bucharest, Department of Railway Vehicles, Splaiul Independenţei 313, Bucharest, Romania
[2]SNTFC CFR Călători S.A., Bdul Dinicu Golescu 38, Bucharest, Romania

Abstract. Rail dampers are mechanical devices mounted at both sides of the rail web aiming to reduce the vibration along the rail. In this way, a shorter length of the rail vibrates effectively and the rolling noise is less intense. In this paper, a continuous model consisting in an infinite Timoshenko beam on multi-elastic layers is adopted for the railway track with rail dampers. The equations of motion are solved using the Green's function method and the frequency-response of UIC 49 rail is derived and analysed in terms of the receptance and decay rate of vibration depending on the possible dimensions of the rail dampers.

1 Introduction

The rolling noise of railway vehicles is an important source of phonic pollution in urban areas, affecting the life of millions of people. Only in Europe it is estimated that approx.12 million persons are exposed to noise levels greater than 55 dB during the day, and approx. 9 million are exposed to over 50 dB overnight [1].

The rolling noise is generated by the structural vibrations of the wheel and rail, induced by the rolling surface's roughness. Very often, the major contributor to the rolling noise is the rail itself, especially within the medium and high frequency range. The wheel component of the rolling noise becomes significant at resonance frequencies over 1500 Hz. Therefore, the mitigation of the rolling noise requires a major focus on that produced by the rail.

A practical solution to reducing the noise level produced by the rails is the rail damper [2]. Usually, the rail dampers are structured as mechanical systems presenting two degree of freedom, and mounted through rubber elements on both sides of the rail web. The rail dampers may take a significant fraction of the rail's vibration and dissipate it, especially at the tuning frequencies, in accordance to the principles presented by the two own-frequencies dynamic absorbing systems. The rate of decay of vibration along the rail is the most important parameter with the strongest influence on the level of noise radiated by the rail [3]. For instance, a doubling of decay rate of vibration along the rail in a particular frequency band leads to the 3 dB reduction of the noise radiated by the rail in that band.

*Corresponding author: trmazilu@yahoo.com

In this work we present the results on the numerical analyses of the vibration decay rate for a rail damper specific to the UIC 49 rail by considering a continuous rail model and the method of Green functions is applied [4].

2 Mechanical model

To investigate the dynamic response of a rail with rail dampers, a distributed parameter model is adopted (Figure 1). This model has the advantage of simplicity achieved by neglecting the distance between the sleepers, which is considered to have a minimal impact on the analysis. This is justified by the observations that the distance between the sleepers has influence on vibration only within a narrow frequency range around the resonance frequency due to the rail bending on sleepers. This range depends on both rail type and distance between sleepers. For example, an UIC49 rail on sleepers spaced to 60 cm presents a resonance due to the bending vibrations of the rail of approx. 880 Hz.

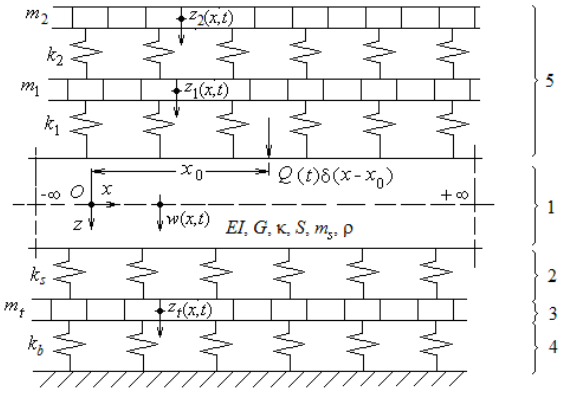

Fig. 1. Mechanical model of the track with rail dampers: 1. Rail; 2. Rail pad; 3. Sleeper; 4. Ballast; 5. Rail damper.

The model comprises a beam placed on an elastic foundation consisting of multiple, successive inertial and elastic layers; their properties are calculated by considering the distance between sleepers. These layers model the effects of the rail pads, sleepers, and ballast prism. Other inertial and elastic layers modelling the rail dampers are attached to the beam (the distributed model).

The rail is modelled as an uniform, infinite Timoshenko beam placed on an elastic foundation consisting of two Winkler elastic model with hysteretic damping, and an intermediate inertial layer in between. The Timoshenko beam model is characterized by several parameters such as: EI – bending stiffness, where E is the longitudinal elastic modulus, and I is the moment of inertia of the beam's cross section; G - transverse elastic modulus; κ – shear coefficient; m_s - specific mass (per length unit), S – cross section area, and ρ – beam density (steel).

The first Winkler elastic layer models the elastic and damping properties of the rail pads. The specific parameters are: the stiffness per length unit, k_s and the loss factor η_s.

The second Winkler elastic layer models the elastic and damping properties of the ballast prism. It is parameterized with the stiffness per length unit, k_b, and the loss factor η_b. It is noted that the ballast prism's inertia was not considered since it only influences the rail's response within the low frequency range.

As per the sleeper's model, owing to their high rigidity, the sleepers are considered an inertial layer of the mass m_t (per length unit) between the rail pad and ballast.

The rail dampers are modelled as two inertial layers of linear mass m_1 and m_2 and two elastic layers of specific rigidity $k_{1,2}$ and loss factors $\eta_{1,2}$.

Applying the principle of D'Alembert, the equations of motion are obtained:

- for rail

$$m_s \frac{\partial^2 w}{\partial t^2} + (k_s + k_1)w + \kappa SG\left(\frac{\partial \theta}{\partial x} - \frac{\partial^2 w}{\partial x^2}\right) - k_s z_t - k_1 z_1 = Q(t)\delta(x - x_o) \tag{1}$$

$$\rho I \frac{\partial^2 \theta}{\partial t^2} + GS\kappa\left(\theta - \frac{\partial w}{\partial x}\right) - EI \frac{\partial^2 \theta}{\partial x^2} = 0 \cdot \tag{2}$$

- for sleepers

$$m_t \frac{\partial^2 z_t}{\partial t^2} + (k_s + k_b) z_t - k_s w = 0 \tag{3}$$

- for rail dampers

$$m_1 \frac{\partial^2 z_1}{\partial t^2} + (k_1 + k_2) z_1 - k_1 w - k_2 z_2 = 0 \,, \tag{4}$$

$$m_2 \frac{\partial^2 z_2}{\partial t^2} + k_2 z_2 - k_2 z_1 = 0 \cdot \tag{5}$$

Next, we investigate the steady-state harmonic behaviour due to an harmonic excitation force of amplitude Q_o and angular frequency ω.

The rail's receptance in the x section due to a harmonic force applied in the x_o position is calculated as:

$$\overline{\alpha}(x, x_o, \omega) = \left(1 - \frac{\omega^2 \rho I}{GS\kappa}\right) G(x, x_o) - \frac{EI}{GS\kappa} \frac{\partial^2 G(x, x_o)}{\partial \xi^2} \,, \tag{6}$$

where G (x, xo) is the Green function of the Timoshenko beam

$$G(x, x_o) = \frac{\gamma_1 \exp\left(-\gamma_2 |x - x_o|\right) - \gamma_2 \exp\left(-\gamma_1 |x - x_o|\right)}{2\gamma_1 \gamma_2 \left(\gamma_1^2 - \gamma_2^2\right) EI} \tag{7}$$

and $\gamma_{1,2}$ are the solutions with the positive real part of the characteristic equation:

$$EI\gamma^4 + \left[\omega^2 \rho I + \frac{EI}{GS\kappa}(\omega^2 m_s - \bar{k}_c - \bar{k}_a)\right]\gamma^2 + (\omega^2 m_s - \bar{k}_c - \bar{k}_a)\left(\frac{\omega^2 \rho I}{GS\kappa} - 1\right) = 0 \,, \tag{8}$$

$$\text{where } \bar{k}_c = \bar{k}_s\left(1 - \frac{\bar{k}_s}{\bar{k}_s + \bar{k}_b - \omega^2 m_t}\right) \tag{9}$$

$$\bar{k}_a = \bar{k}_1\left(1 - \frac{\bar{k}_1(\bar{k}_2 - \omega^2 m_2)}{m_1 m_2 \omega^4 - \left[m_1 \bar{k}_2 + m_2(\bar{k}_1 + \bar{k}_2)\right]\omega^2 + \bar{k}_1 \bar{k}_2}\right) \tag{10}$$

Where $\bar{k}_{s,b} = k_{s,b}(1+\mathrm{i}\eta_{s,b})$, $\bar{k}_{1,2} = k_{1,2}(1+\mathrm{i}\eta_{1,2})$ with $\mathrm{i}^2 = -1$.

The rail decay rate of the vibrations along the rail can be calculate

$$R(x,\omega) = \frac{20}{x}\lg\frac{\left|\overline{W}(0)\right|}{\left|\overline{W}(x)\right|} = \frac{20}{x}\lg\frac{\left|\bar{\alpha}(0,0,\omega)\right|}{\left|\bar{\alpha}(x,0,\omega)\right|} \text{ [dB/m].} \tag{11}$$

3 Numerical application

This section shows the results obtained with the above model. The following parameters are considered: UIC 49 rail: m_s = 49.39 kg/m, EI = 3.8136 MNm^2, GS = 509.652 MN, □ = 0.4; concrete sleeper: m_t = 208 kg/m; rail pad stiffness: elastic – k_s = 133.3 MN/m^2, stiff –k_s = 583.3 MN/m^2, □$_s$ = 0.15; ballast stiffness: k_b = 70 MN/m^2, □$_b$ = 0.30; rail damper: $m_1 = m_2$ = 5 kg/m, k_1 = 197.39 MN/m^2, k_2 = 7.8957 MN/m^2, □$_1$ = 0.15, □$_2$ = 0.20.

The natural frequencies of the rail damper can be calculated with the equation

$$\nu_{1,2} = \sqrt{\frac{\nu_{1o}^2 + (1+\mu)\nu_{2o}^2 \mp \sqrt{\left[\nu_{1o}^2 + (1+\mu)\nu_{2o}^2\right]^2 - 4\nu_{1o}^2\nu_{2o}^2}}{2}}, \tag{12}$$

Where $\nu_{1o,2o} = \frac{1}{2\pi}\sqrt{\frac{k_{1,2}}{m_{1,2}}}$ are the uncoupled natural frequencies and $\mu = m_2/m_1$ – the masses ratio.

Figure 2 shows the influence of the rail dampers on the rail receptance for both the undamped case and the damped case for the situation where the rail pad has elastic properties. In the case of an undamped rail, it is noted that the response resembles that of a two-degree o freedom system, being dominated by two resonance frequencies at 82 Hz and 294 Hz, respectively. The low resonance frequency is given by the elasticity of the ballast, and the high resonance frequency of the rail pad. Among these, we have an anti-resonance frequency of 157 Hz. This anti-resonant behaviour is due to the effect of the dynamic absorber of the sleepers.

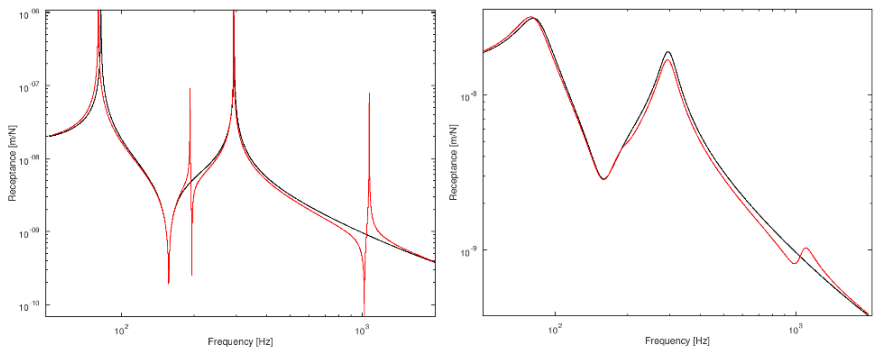

Fig. 2. Rail receptance on elastic rail pad: left – undamped; right – damped; black – rail without rail dampers; red – rail with rail dampers.

Regarding the rail dampers, calculations from equation (12) show that their natural frequencies are at 196 and 1021 Hz, only bit different from the actual frequencies of the decoupled bodies (200 and 1000 Hz). It is noted that due to the presence of the rail dampers, the rail now has 4 natural frequencies, two of them are close to the frequencies

obtained on the undamped rail at 80 Hz and 292.5 Hz, and both are closed to the natural frequencies of the rail damper - at 192.5 and 1070 Hz.

The rail with dampers has an anti-resonant mode at the same frequency as a undamped rail. Beside this, there are two more anti-resonance frequencies corresponding to the resonance frequencies which are introduced by the rail dampers at 196 and 1020.5 Hz, respectively. In case of amortization, the rail receptance has the same main characteristics: the frequency domains dominated by the resonance or anti-resonance response occur, but the response is the approximate form to the dominant frequencies. The influence of the rail dampers is mainly observed around the high resonance frequency where the rail response is lower due to the rail dampers. At higher frequencies than the high frequency of the rail damper (over 1000 Hz), the rail response is higher than in the case of the rail without rail dampers.

The rail receptance shows similar characteristics when the rail pad is rigid (see Figure 3). The rail without rail dampers has resonance frequencies at 83 and 618 Hz, and the anti-resonance frequency of 285 Hz. If the rail is provided with rail dampers, we have the resonance frequencies: at 81 Hz and 590 Hz due to the ballast and the rail pad, respectively, and the 198 Hz and 1084 Hz due to the rail dampers. There are also anti-resonance frequencies at 196 and 1021 Hz. The damping effects rail response, especially around the resonance and anti-resonance frequencies. The low resonance frequency of the rail damper is faded due to the damping. The rail-rail dampers response is reduced at frequencies higher than the high resonance frequency (590 Hz). Instead, at frequencies higher than the high frequency of the rail damper (1084 Hz), the rail response is higher.

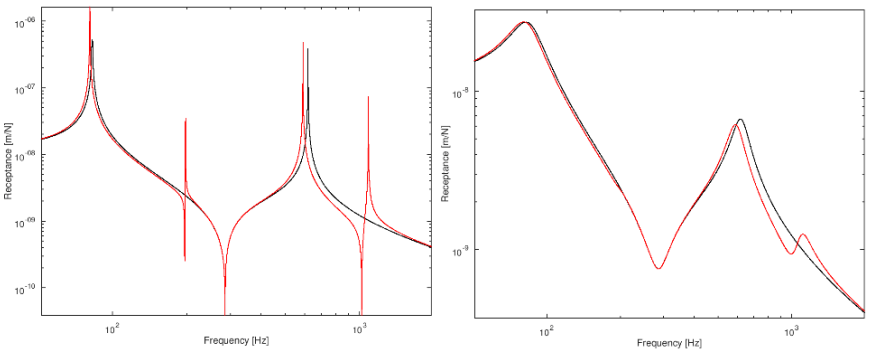

Fig. 3. Rail receptance on stiff rail pad: left – undamped; right – damped; black – rail without rail dampers; red – rail with rail dampers.

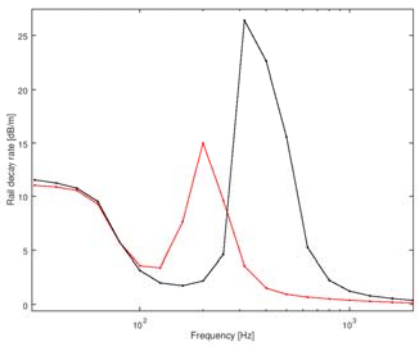

Fig. 4. Rail decay rate for rail without rail dampers: black - stiff rail pad; red – elastic rail pad.

Figure 4 shows the rail decay rate vibration depending on the frequency for the elastic rail pad and stiff rail pad (without rail dampers). The two curves are similar. At frequencies lower than 100 Hz, the attenuation rate does not depend on the stiffness of the rail pad. It decreases as the frequency increases to a minimum between of 100 to 200 Hz. The highest decay rate is at the anti-resonance frequency after which it decreases a lot. It can be seen that between 100 and 250 Hz, the rail decay rate is higher if the rail pad is elastic. Instead, at frequencies greater than 250 Hz, the rail decay rate is higher in the case of the stiff rail pad.

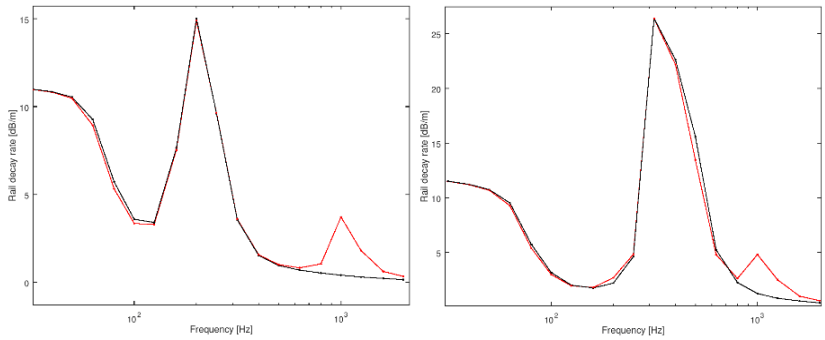

Fig. 5. Rail decay rate: left – elastic rail pad; right – stiff rail pad; black – rail without rail dampers; red – rail with rail dampers.

Figure 5 shows the impact of the rail dampers on the rail decay rate of the vertical vibration of the rail. It is noted that the decay rate of the rail is influenced by the rail dampers significantly at the high resonance frequency of the rail dampers, respectively 1000 Hz.

4 Conclusions

In this paper the influence of the rail dampers on the rail response is investigated using the Green function method. The track is consisting of a Timoshenko beam with continuous elastic foundation. Continuous equivalent models with two elastic layers are used for the rail dampers. Rail receptance and the decay rate of the vertical vibration were calculated.

The rail dampers reduce the rail response around the high resonance frequency given by the rail pad. The rail dampers increase the rail decay rate in the frequency range around the high resonance frequency of the rail dampers.

This work was supported by a grant of the Romanian National Authority for Scientific Research and Innovation, CNCS/CCCDI - UEFISCDI, project number PN-III-P2-2.1-PED-2016-0748, within PNCDI III.

References

1. M. Dumitriu, C. I. Cruceanu, J. of Eng. Science and Tech. Review, **10**, 6 (2017)
2. D. J. Thompson, J. Sound Vibr. **311**, 824-842 (2008)
3. D. J. Thompson, C.J.C. Jones, T.P. Waters, D. Farrington, Appl. Ac. **68**, 43-57 (2007)
4. T. Mazilu, Proc. Rom. Acad., Ser. A **10**, 139-150 (2009)